AGU PUBLICATIONS

Geophysical Research Letters

RESEARCH LETTER

10.1002/2013GL059185

Key Points:
- Short-term atmospheric blocking over Greenland contributes to melt episodes
- Associated temperature anomalies are equally important for the melt
- Duration and strength of blocking events contribute to surface melt intensity

Supporting Information:
- Readme
- Text S1
- Figure S1
- Figure S2
- Figure S3
- Figure S4

Correspondence to:
S. Häkkinen,
Sirpa.Hakkinen@nasa.gov

Citation:
Häkkinen, S., D. K. Hall, C. A. Shuman, D. L. Worthen, and N. E. DiGirolamo (2014), Greenland ice sheet melt from MODIS and associated atmospheric variability, *Geophys. Res. Lett.*, *41*, 1600–1607, doi:10.1002/2013GL059185.

Received 31 DEC 2013
Accepted 7 FEB 2014
Accepted article online 12 FEB 2014
Published online 10 MAR 2014

This is an open access article under the terms of the Creative Commons Attribution-NonCommercial-NoDerivs License, which permits use and distribution in any medium, provided the original work is properly cited, the use is non-commercial and no modifications or adaptations are made.

Greenland ice sheet melt from MODIS and associated atmospheric variability

Sirpa Häkkinen[1], Dorothy K. Hall[1], Christopher A. Shuman[1,2], Denise L. Worthen[1,3], and Nicolo E. DiGirolamo[1,4]

[1]NASA Goddard Space Flight Center, Greenbelt, Maryland, USA, [2]Joint Center for Earth Systems Technology (JCET), University of Maryland, Baltimore County, Baltimore, Maryland, USA, [3]Wyle Information Systems, LLC, Lanham, Maryland, USA, [4]Science Systems and Applications Inc., Lanham, Maryland, USA

Abstract Daily June-July melt fraction variations over the Greenland ice sheet (GIS) derived from the Moderate Resolution Imaging Spectroradiometer (MODIS) (2000–2013) are associated with atmospheric blocking forming an omega-shape ridge over the GIS at 500 hPa height. Blocking activity with a range of time scales, from synoptic waves breaking poleward (<5 days) to full-fledged blocks (≥5 days), brings warm subtropical air masses over the GIS controlling daily surface temperatures and melt. The temperature anomaly of these subtropical air mass intrusions is also important for melting. Based on the years with the greatest melt (2002 and 2012) during the MODIS era, the area-average temperature anomaly of 2 standard deviations above the 14 year June-July mean results in a melt fraction of 40% or more. Though the summer of 2007 had the most blocking days, atmospheric temperature anomalies were too small to instigate extreme melting.

1. Background

Recently, a data record of the clear-sky ice surface temperature (IST) of the Greenland ice sheet (GIS) was developed using Moderate Resolution Imaging Spectroradiometer (MODIS) data from the Terra and Aqua satellites [*Hall et al.*, 2012]. The record extends from March 2000 through the present, providing daily and monthly average IST, and melt maps at 6.25 × 6.25 km resolution. Based on this MODIS IST record, years experiencing major melt (defined as melt covering 80% or more of the ice sheet surface) have occurred twice since 2000 [*Hall et al.*, 2013]. The extreme melt year of 2012 had two separate intense melt events. The most unusual melt event occurred on 11–12 July 2012 and was unprecedented during this and the previous century, covering ~99% of the ice sheet surface including areas >3000 m at Summit Station (Figure 1a) according to data from multiple satellite sensors [*Nghiem et al.*, 2012]. Melt this extensive had not occurred since 1889 (+/−1 year) according to ice core records [*Nghiem et al.*, 2012; *Clausen et al.*, 1988; *Alley and Anandakrishnan*, 1995]. Another large melt event occurred on 29 July 2012, where ~79% of the surface experienced some melt according to data from multiple satellite sensors [*Nghiem et al.*, 2012]. In 2002 an intense melt event occurred on 29 June to 2 July. The cumulative melt during the 2002 melt season covered > 87% of the ice sheet surface according to MODIS IST clear-sky data [*Hall et al.*, 2013].

The negative phase of the North Atlantic Oscillation (NAO), with a high-pressure anomaly over the GIS, has previously been implicated [*Mote*, 1998] in enhancing melting of the surface of the GIS. Also, the 2012 melt event was associated with a high-pressure ridge over the GIS [*Nghiem et al.*, 2012; *Tedesco et al.*, 2013; *Hanna et al.*, 2013]. A high-pressure ridge brings relatively warm southerly winds over the western flank of the ice sheet causing widespread surface melting [*Nghiem et al.*, 2012]. A high-pressure ridge also represents atmospheric blocking, which is a long-lived (5 days or longer) atmospheric circulation system with strong meridional flows embedded within the latitude belt of westerlies [*Tibaldi and Molteni*, 1990; *Tibaldi et al.*, 1997] (definition also shown in the supporting information). Blocking in the North Atlantic sector is usually associated with the negative phase of the NAO, and known as a Greenland Blocking Episode (GBE) [*Fang*, 2004; *Woollings et al.*, 2008]. GBEs have a continuum of behavior, from being relatively frequent but weak events, to longer and stronger events that better conform to the conventional interpretation (and definition) of midlatitude blocking. Here we are also interested in shorter than 5 day blocking activity, because we anticipate that even a 2 day burst of warm subtropical air over the GIS could lead to melting. These short events are called local and instantaneous blocking (LIB), if on any day a longitude is blocked based on the

©2014. The Authors.

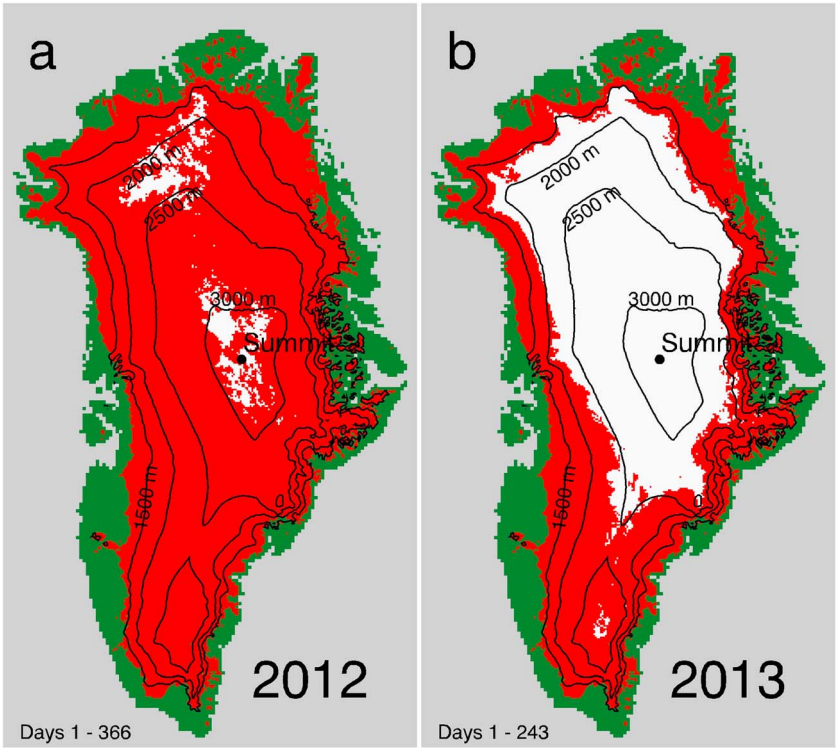

Figure 1. Extent of melt on the Greenland ice sheet for (a) 1 January to 31 December 2012 (days 1–366) and (b) 1 January to 30 August 2013 (days 1–243) as determined from MODIS-derived melt maps. A maximum of ~95% of the ice sheet surface (shaded red) experienced some melt in 2012 and only ~49% of the ice sheet surface experienced some melt in 2013. White represents no melting (according to MODIS), and green represent non-ice covered land areas. The location of Summit, mentioned in the text, is shown. Elevation contours are shown at 1500, 2000, 2500, and 3000 m.

reversal of the gradient in the 500 hPa geopotential height field [*Tibaldi and Molteni*, 1990; *Tyrlis and Hoskins*, 2008]. Some of the LIBs belong to GBEs if they are spatially stationary for 5 days or more.

We focus here on daily variability of melt and atmospheric conditions instead of seasonal variability. Both LIBs and GBEs are accompanied by warm air temperatures and we will show that are both capable of initiating ice sheet melt. We will also show that daily air temperature at about 5 km height, about 2 km above the ice sheet, varies in-phase with MODIS IST in June and July, the months most likely to have intense melt events. Finally, we will discuss the relationship between GIS melt and blocking and associated temperature variability.

2. Data and Methods

We use the MODIS clear-sky IST data record (2000–2013) to calculate GIS melt. For the retrieval of MODIS clear-sky IST, a split-window technique is used, where "split-window" refers to the brightness-temperature difference in the 11–12 m atmospheric window. This technique allows for the correction of atmospheric effects primarily due to water vapor. The technique was first used to determine IST in the Arctic with advanced very high resolution radiometer (AVHRR) data on NOAA polar-orbiting satellites [*Key and Haefliger*, 1992] and later adapted for use with MODIS.

Using MODIS IST we quantify number of melt days and areal extent of melt for each year of the study (Figure 1). Melt that may occur beneath cloud cover will not be detected using this method. Cloud cover is determined from the standard MODIS cloud mask of *Ackerman et al.* [1998]. To partly compensate for the effects of cloud cover, for this work we employ a cloud-gap filling algorithm (see supporting information) to minimize the impact of cloud cover. As in previous work [*Hall et al.*, 2012, 2013], we also classify an IST grid cell as "melt" if the surface temperature is ≥ −1°C. This temperature has been found to be representative of melting conditions over the GIS, in consideration of MODIS IST measurement uncertainty of +/−1°C at the

©2014. The Authors.

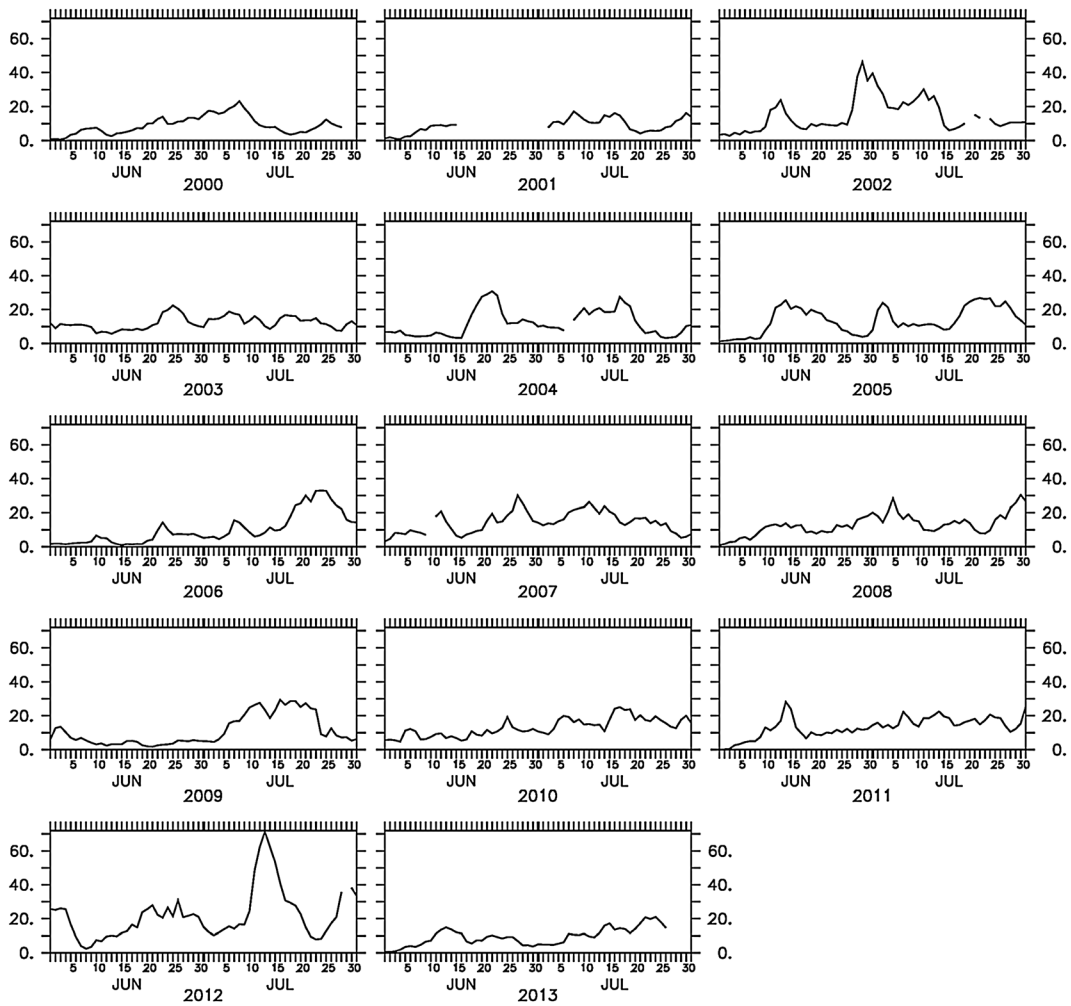

Figure 2. Total melt area percentage over the area of the Greenland ice sheet (*y* axis, %) for June and July for each year, 2000–2013, derived from daily MODIS IST data.

high (near 0°C) values of IST over ice [*Hall et al*., 2008]. We use daily melt to infer associated atmospheric conditions on a daily basis.

We utilize the National Centers for Environmental Prediction/National Center for Atmospheric Research (NCEP/NCAR) reanalysis data [*Kalnay et al*., 1996] to analyze daily average 500 hPa geopotential height (Z500) and temperature (T500), and daily average air temperature at 2 m (T2m), all of which are derived from 6-hourly data. The reanalysis data resolution is 2.5° × 2.5°. To compute area-average temperatures, T500 and T2m were interpolated to the MODIS IST grid of 6.25 km and constrained by the MODIS ice sheet mask. Blocking is computed by searching reversals of the gradient in the daily (average) 500 hPa geopotential height at each grid longitude and latitude in a region 20°W–60°W, 50°N–85°N instead of over fixed latitudes [*Tibaldi and Molteni*, 1990] (supporting information). We record both LIBs and GBEs. Additionally, the NAO indices are retrieved from the NOAA/Climate Prediction Center.

3. Results

The maximum area that experienced at least 1 day of melt during the melt period in 2012 and 2013 is shown in Figures 1a and 1b, as determined from the MODIS IST product. The contrast in the extent of melt between 2012 and 2013 is striking, with MODIS-derived melt covering ~95% of the ice sheet surface in 2012 and ~49% in 2013. (By combining MODIS with microwave sensors that can detect melt through cloud cover, the 2012 melt extent actually covered 99% of the ice sheet surface [*Nghiem et al*., 2012] as discussed

©2014. The Authors.

Table 1. NAO Index Versus the Total GIS Melt Percentage From MODIS[a]

Year	Melt (%)	June NAO Index	July NAO Index
2000	*54*	*neutral*	*negative*
2001	*51*	*weak negative*	*weak negative*
2002	87	positive	positive
2003	*54*	*~neutral*	*~neutral*
2004	71	negative	positive
2005	62	neutral	negative
2006	62	positive	positive
2007	58	negative	negative
2008	*53*	*negative*	*negative*
2009	63	negative	strong negative
2010	*57*	*negative*	*negative*
2011	64	negative	negative
2012	95	strong negative	negative
2013 (days 1–243)	*49*	*positive*	*positive*

[a]MODIS data updated from *Hall et al*. [2013]; NAO index from NOAA/Climate Prediction Center. Minimal melt years are in italics.

previously.) Using available atmospheric NCEP/NCAR reanalysis fields, we can illuminate the differences in the synoptic regime between these two consecutive years and illustrate the relationship between atmospheric patterns and melt over the entire 2000–2013 melt season MODIS IST record on the daily time scale.

The MODIS-derived daily melt area is shown in Figure 2 for June and July. MODIS melt data are not plotted if the gap-filled cloudiness is >11% of the ice sheet area. (This cutoff of 11% was determined by visual scanning of the cloudiness data and thus appeared to be a logical cutoff value. Though it is a subjective choice, the results do not change significantly if we select a cutoff number between 10 and 15%.) Daily percent melt fractions do not reach as high as quoted above for the cumulative area of melt because the melt location varies day-to-day. The 14 year June-July mean daily melt percentage is 13% and the standard deviation (SD) is 8% (based on 834 daily values excluding MODIS data gaps). The maximum 1 day percent melt of 71% (clear-sky) occurred on 13 July 2012. The only other days with melt percentage over 40% occurred on 29 June 2002 (46%), and 11–12 July (49% and 62%), and 14–16 July (63%, 54%, and 41%) 2012. Low melt years in the MODIS record are the following: 2000 (potentially 2001; based on atmospheric temperatures, shown later), 2003, 2008, 2010, and 2013. In each of the low melt years, the average June-July melt fraction was less than or equal to the 14 year June-July mean. The low melt years 2000 (2001), 2003, 2008, and 2010 occurred during a negative or neutral NAO phase (Table 1 and the NAO index in Figure S1 in the supporting information), which should have favored increased melt. The low melt in 2013, however, was associated with a positive NAO index as expected. Another example of NAO with a "wrong sign" is the extensive melt year 2002, which was dominated by a positive phase of the NAO (Table 1). Thus, the GIS melt-NAO relationship is not consistent during the MODIS years, and when using daily NAO index data, the NAO index explains only 15% of the GIS melt variance.

To identify the atmospheric pattern associated with the intense melt events in the MODIS record on a daily time scale, we analyzed daily June-July Z500 and T500 fields for 2000–2013. We composited these fields based on the daily anomaly in the MODIS melting fraction as an index time series. The daily MODIS melt anomalies were derived, and the MODIS melt index was formed, by normalizing the anomaly time series by its SD:

$$\text{Melt index} = [(\text{daily melt}) - (\text{mean_daily_melt})]/\text{SD}, \text{where mean_daily_melt} = 13\%; \text{ and SD} = 8\%$$

We selected Z500 and T500 fields from the days when the melt index exceeded 1 SD (in absolute terms). This approach groups the selected Z500 and T500 fields to positive melt index anomaly days (120 fields) and negative melt index anomaly days (113 fields). The composited fields show that the large melt events are associated with a meander in the Z500 field resembling an Omega-block (Ω pattern, see Figures 3a and 3b) over Greenland, with lows flanking the high-pressure domain. Minimal melt anomalies are associated with a more-or-less zonal flow over the ice sheet (Figures 3c and 3d). The warmest intrusion of the subtropical air masses envelopes both western and eastern flanks of the GIS south of about 75°N. However, the influence of

©2014. The Authors.

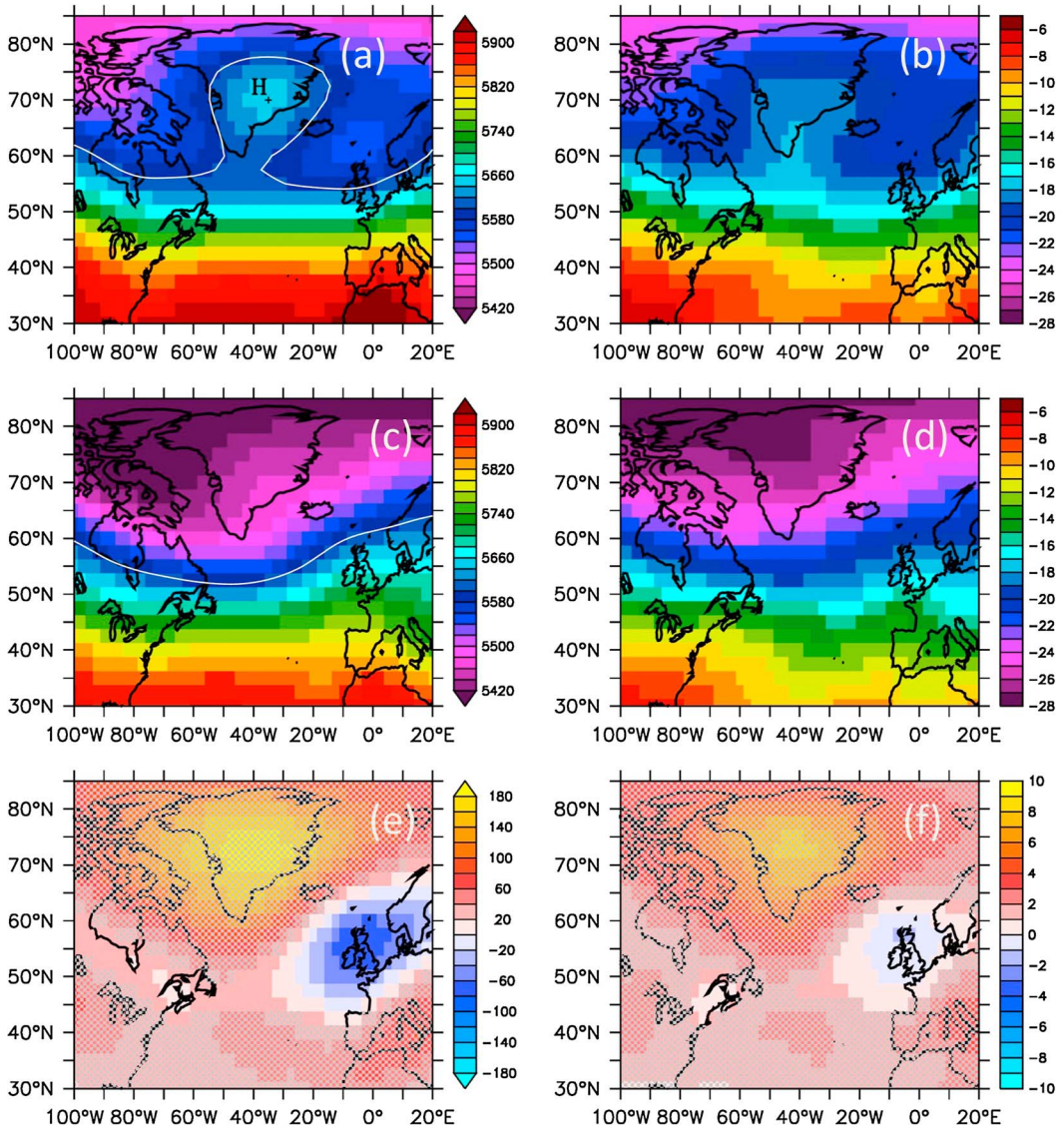

Figure 3. The 2000–2013 composite of 500 hPa (a, c, and e) geopotential heights (meters) and (b, d, and f) temperatures (°C) when the MODIS melt (shown in Figure 2) anomaly is stronger than +1 standard deviation (Figures 3a and 3b), and less than −1 standard deviation (Figures 3c and 3d). The difference is shown in Figures 3e and 3f for Figures 3a–3c and Figures 3b–3d, respectively. In Figures 3a and 3c, Z500 = 5600 m is drawn as a white contour; also, in Figure 3a, maximum Z500 = 5647 m is marked. The cross-hatched values denote differences that are significant at the 99% level.

blocking on temperatures extends far outside this core region as a subtropical regime has moved northward pushing cold air masses far into the Arctic.

While it is obvious that the composited patterns corresponding to high and low melt events are significantly different, we show also the difference fields of Z500 and T500 with cross hatching for areas significant at the 99% level (Figures 3e and 3f). The Z500 difference field has a strong positive anomaly over Greenland but lacks a strong negative height field anomaly at the midlatitudes across the North Atlantic, typical of the negative NAO [*Barnston and Livezey*, 1987]. This is consistent with a weak relationship between MODIS melt area variations and the NAO index. Comparing the blocked flow with the zonal flow (Figures 3c and 3d), the upper air temperature anomaly over Greenland reaches almost 10°C during these subtropical air mass intrusions.

Another approach to show the impact of the subtropical intrusions is to analyze the daily area-average MODIS IST, T2m, and T500 variability. We created an anomaly time series for each of these quantities and then

©2014. The Authors.

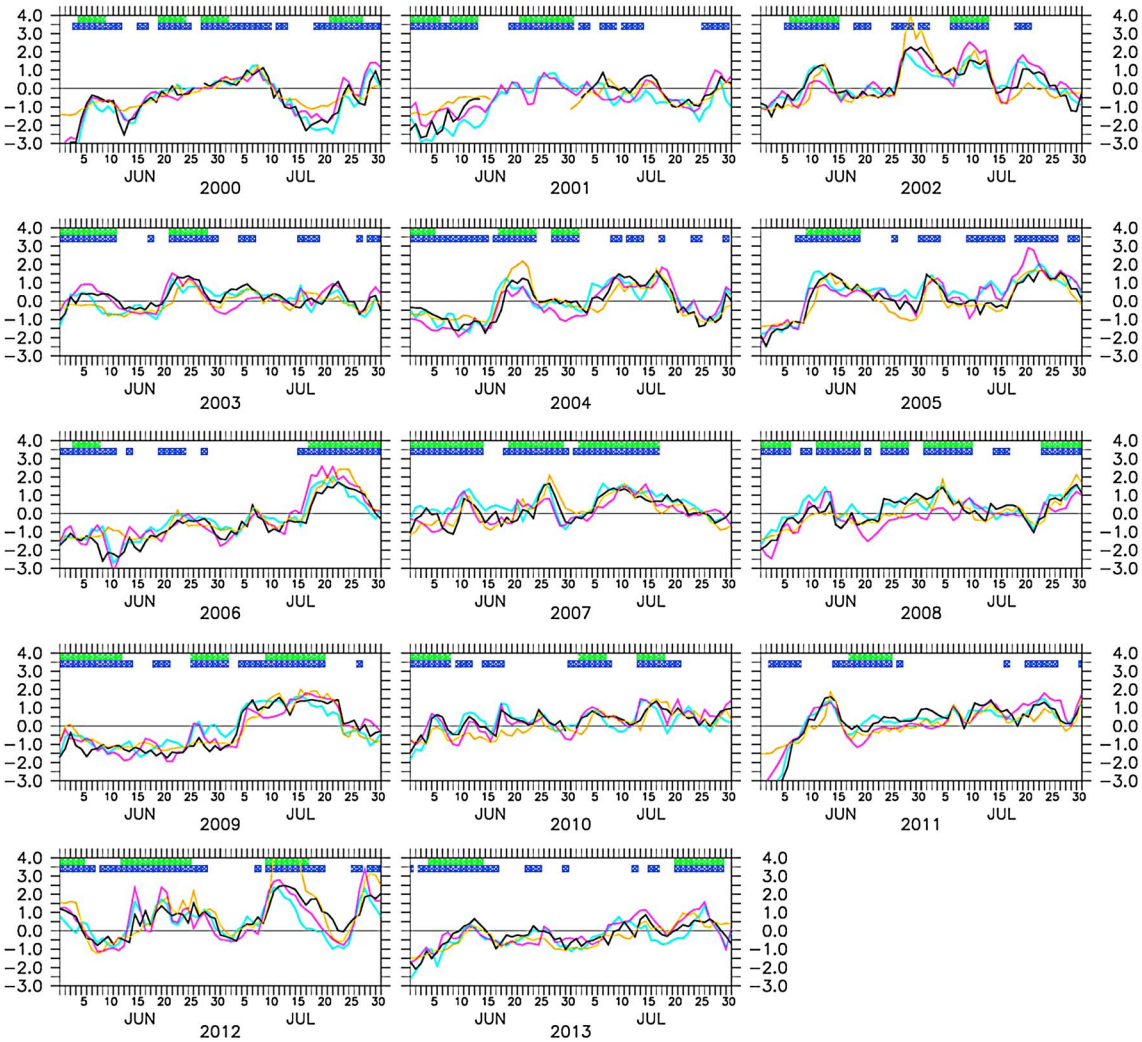

Figure 4. Area-average MODIS IST (black), T2m (pale blue), and T500 (pink) temperature anomalies and MODIS melt anomaly (in orange) (referenced to 14 year June-July averages), which are then normalized by their individual standard deviation (*y* axis measures SDs). During 2012 summer normalized melt anomaly reached 7 standard deviations (beyond the *y* axis upper limit). Blocking days (green bars) and all days when the 500 hPa geopotential height gradient is reversed (blocking + wave breaking events, blue bars) are shown for June–July, 2000–2013. The blocking and wave breaking events do not always start and end at the same day, because not all gradient reversals occurred at the same locations on the ice sheet (and lasting 5 days).

normalized them by their SD (anomaly and SD with respect to 2000–2013 June-July average, SD based on all days in each time series) giving SDs of 2.5°C, 2.1°C, and 2.9°C for IST, T2m, and T500, respectively. The normalized area-average MODIS IST, T2m, and T500 are displayed in Figure 4 for June-July of each year. Also, the normalized MODIS melt area anomaly is shown. The daily temperature variations from the ice sheet surface to the upper atmosphere, about 2 km higher than Summit Station, vary in-phase and in most years with similar normalized amplitude. Previously, *Box and Cohen* [2006] showed this relationship between surface and tropospheric temperatures on seasonal and annual time scales from the coastal radiosonde measurements. (In their data, the relationship was not as strong in the stations on the eastern side of Greenland.) The tight coupling between the surface and upper atmosphere shows that during the period of high insolation, the only preconditioning necessary for melt is an intrusion of subtropical air. Here we note that this relationship is the strongest for June-July; adding August to the time series does not affect the timing of the variations but changes slightly the relationship between surface and upper air temperatures by increasing the differences in amplitudes (not shown).

In Figure 4 we have also identified days of LIBs (there is at least one longitude that is blocked at least 1 day), of which some belong to GBEs, if the condition of Z500 gradient reversal existed at least in one grid point for 5

©2014. The Authors.

days or more. Considering first the temperature anomalies above 1.5 SDs, these warm events occur when they overlap with LIBs and/or GBEs with the spatial pattern depicted in Figures 3a and 3b. There are two exceptions: on 16–18 July 2004 and 13–15 June 2011, with GIS melt reaching 28–31% (~2 SDs above 14 year June-July mean of 13%; SD = 8%). In both cases the Z500 gradient reversal occurred but the westerlies north of the blocking high were too weak to classify them as LIBs by our definition; however, the circulation associated with their Z500 pattern favored bringing subtropical air masses over Greenland (Figure S2).

In the case of weaker warming events with 1–1.5 SDs, the warming-blocking relationship also holds with three exceptions—23 July 2003, 7–8 July 2011, and 13–15 July 2011. During these three events, the GIS melt percentage either did not reach above 1 SD (15% in 2003) or did so marginally (22% in 2011). These three marginal warming/melting events are not classifiable by our blocking definition because they had complex patterns, involving a cutoff low with or without a ridge over the GIS (Figure S3).

Only a few LIBs/GBEs occurring in the first half of June will result in a large melt event. If melt occurs, the temperature anomaly, whether surface or upper air, has to be about 1.5 SDs above the summer average (e.g., in 2002, 2005, and 2012). Furthermore, we can estimate that area-average temperature anomalies of almost 2 SDs above the summer average are needed to reach a melt fraction over 40% as happened in 2002 and 2012 (Figures 2 and 4). Once temperature anomalies reach 2 SDs (~5–6°C), the melt amplifies almost exponentially (Figure S4). Even if the blocking activity does not lead to a melt event, the temperatures nevertheless show a warming tendency during those days.

Figure 4 shows that June-July 2007 had the most blocking days but did not have the largest melt, although 2007 has been identified as a large melt year in a seasonal sense [*Mote*, 2007; *Tedesco*, 2007]. The melt was largely confined to the southern part of the ice sheet, but Figure 4 also shows that the 2007 area-average temperature anomalies barely reached 1.5 SDs (only once in the end of June). If compared especially to 2012 with a long-lasting anomaly of 2–2.5 SDs at the peak melt 10–15 July, the potential of 2007 to be an extreme melt year evaporated due to the weak temperature anomalies in the subtropical air masses. We conclude that the total number of days with blocking over Greenland does not necessarily correlate with the most melt area, but the associated temperature anomalies are equally, if not more, important.

4. Summary

Previously studies have shown that blocking can be associated with increased Greenland ice sheet melt on seasonal time scales [e.g., *Fettweis et al*., 2013], and here we show, using MODIS and atmospheric reanalysis (NCEP/NCAR) data, that the relationship holds also on a daily time scale. Our analysis of all 14 melt seasons (2000–2013) shows that blocking that occurs in a range of time scales, from short-term blocking activity ($<$5 days) (LIBs) to full-fledged GBEs (blocking for 5 days or longer), can bring warm subtropical air masses over the GIS to instigate melt. Despite the overall close relationship between GBEs/LIBs and ice sheet melt, not all blocking activity leads to melt as exemplified in the summer 2007 which had the most June-July blocking days during the period 2000–2013. In addition, the surface and upper air temperature anomalies, computed here from area-average temperatures, play an important role during the largest melt years such that temperature anomalies have to reach almost 2 standard deviations to result in a melt area above 40% as happened in 2002 and 2012. In the case of summer 2007, the temperature anomalies barely reached 1.5 standard deviations; hence, the summer 2007 melt did not achieve extreme melt status.

Acknowledgments
We thank the NASA Cryospheric Sciences Program and the NASA Physical Oceanography Program for support. We are grateful for the constructive comments by Son Nghiem and one anonymous reviewer and by the Editor, Julienne Stroeve.

The Editor thanks Xuanji Wang and an anonymous reviewer for their assistance in evaluating this paper.

References

Ackerman, S. A., K. I. Strabala, P. W. P. Menzel, R. A. Frey, C. C. Moeller, and L. E. Gumley (1998), Discriminating clear sky from clouds with MODIS, *J. Geophys. Res.*, *103*, 32,141–32,157, doi:10.1029/1998JD200032.

Alley, R., and S. Anandakrishnan (1995), Variations in melt-layer frequency in the GISP2 ice core: Implications for Holocene summer temperatures in Greenland, *Ann. Glaciol.*, *21*, 64–70.

Barnston, A. G., and R. E. Livezey (1987), Classification, seasonality and persistence of low-frequency atmospheric circulation patterns, *Mon. Weather Rev.*, *115*, 1083–1126.

Box, J. E., and A. E. Cohen (2006), Upper-air temperatures around Greenland 1964–2006, *Geophys. Res. Lett.*, *33*, L12706, doi:10.1029/2006GL025723.

Clausen, H. B., N. S. Gundestrup, S. J. Johnsen, R. Bindschadler, and J. Zwally (1988), Glaciological investigations in the Crete area, central Greenland: A search for a new deep-drilling site, *Ann. Glaciol.*, *10*, 10–15.

Fang, Z.-F. (2004), Statistical relationship between the Northern Hemisphere sea ice and atmospheric circulation during wintertime, in *Observation, Theory and Modeling of Atmospheric Variability*, edited by X. Zhu, pp. 131–141, World Scientific Series on Meteorology of East Asia. World Scientific Publishing Company, Singapore.

 ©2014. The Authors.

Fettweis, X., E. Hanna, C. Lang, A. Belleflamme, M. Erpicum, and H. Gallée (2013), Important role of the mid-tropospheric atmospheric circulation in the recent surface melt increase over the Greenland ice sheet, *Cryosphere*, *7*, 241–248.

Hall, D. K., J. E. Box, K. A. Casey, S. J. Hook, C. A. Shuman, and K. Steffen (2008), Comparison of satellite-derived ice and snow surface temperatures over Greenland from MODIS, ASTER, ETM1 and in-situ observations, *Remote Sens. Environ.*, *112*, 3739–3749, doi:10.1016/j.rse.2008.05.007.

Hall, D. K., J. C. Comiso, N. E. DiGirolamo, C. A. Shuman, J. R. Key, and L. S. Koenig (2012), A satellite-derived climate-quality data record of the clear-sky surface temperature of the Greenland ice sheet, *J. Clim.*, *25*(14), 4785–4798.

Hall, D. K., J. C. Comiso, N. E. DiGirolamo, C. A. Shuman, J. E. Box, and L. S. Koenig (2013), Variability in the surface temperature and melt extent of the Greenland ice sheet from MODIS, *Geophys. Res. Lett.*, *40*, 1–7, doi:10.1002/grl.50240.

Hanna, E., J. M. Jones, J. Cappelen, S. H. Mernild, L. Wood, K. Steffen, and P. Huybrechts (2013), The influence of North Atlantic atmospheric and oceanic forcing effects on 1900–2010 Greenland summer climate and ice melt/runoff, *Int. J. Climatol.*, *459*(33), 862–880, doi:10.1002/joc.3475.460.

Kalnay, E., et al. (1996), The NCEP/NCAR 40-year reanalysis product, *Bull. Am. Meteorol. Soc.*, *77*, 437–471.

Key, J., and M. Haefliger (1992), Arctic ice surface temperature retrieval from AVHRR thermal channels, *J. Geophys. Res.*, *97*(D5), 5885–5893.

Mote, T. L. (1998), Mid-tropospheric circulation and surface melt on the Greenland ice sheet. Part 1: Atmospheric teleconnections, *Int. J. Climatol.*, *18*, 111–129.

Mote, T. L. (2007), Greenland surface melt trends 1973–2007: Evidence of a large increase in 2007, *Geophys. Res. Lett.*, *34*, L22507, doi:10.1029/2007GL031976.

Nghiem, S. V., D. K. Hall, T. L. Mote, M. Tedesco, M. Albert, K. Keegan, C. A. Shuman, N. E. DiGirolamo, and G. Neumann (2012), The extreme melt across the Greenland ice sheet in 2012, *Geophys. Res. Lett.*, *39*, L20502, doi:10.1029/2012GL053611.

Tedesco, M. (2007), Snowmelt detection over the Greenland ice sheet from SSM/I brightness temperature daily variations, *Geophys. Res. Lett.*, *34*, L02504, doi:10.1029/2006GL028466.

Tedesco, M., X. Fettweis, T. Mote, J. Wahr, P. Alexander, J. E. Box, and B. Wouters (2013), Evidence and analysis of 2012 Greenland records from spaceborne observations, a regional climate model and reanalysis data, *Cryosphere*, *7*, 615–630, doi:10.5194/tc-7-615-2013.

Tibaldi, S., and F. Molteni (1990), On the operational predictability of blocking, *Tellus A*, *42*, 343–365, doi:10.1034/j.1600-0870.1990.t01-2-00003.x.

Tibaldi, S., F. D'Andrea, E. Tosi, and E. Roeckner (1997), Climatology of Northern Hemisphere blocking in the ECHAM model, *Clim. Dyn.*, *13*, 649–666.

Tyrlis, E., and B. J. Hoskins (2008), Aspects of a Northern Hemisphere atmospheric blocking climatology, *J. Atmos. Sci.*, *65*, 1638–1652.

Woollings, T. J., B. J. Hoskins, M. Blackburn, and P. Berrisford (2008), A new Rossby wave-breaking interpretation of the North Atlantic Oscillation, *J. Atmos. Sci.*, *65*, 609–626.

©2014. The Authors.